

REMOTELY SENSED ESTIMATION OF RICE NITROGEN CONCENTRATION FOR FORCING CROP GROWTH MODELS

USO DI DATI TELERILEVATI PER LA STIMA DELLA CONCENTRAZIONE DI AZOTO
PER IL FORCING DI MODELLI AGRONOMICI

Daniela Stroppiana^{1*}, Mirco Boschetti¹, Pietro Alessandro Brivio¹, Stefano Bocchi²

¹ CNR-IREA, Institute for Electromagnetic Sensing of the Environment, Via Bassini 15, 20133 Milano, Italy

² Department of Crop Science, Section of Agronomy, University of Milano, Via Celoria 2, 20133 Milano, Italy

* Corresponding Author: Tel. +39 02 23699.454; E-mail: stroppiana.d@irea.cnr.it; Fax +39 02 23699300

Received 28/8/2006 – Accepted 1/12/2006

Abstract

Monitoring crop conditions and assessing nutrition requirements is fundamental for implementing sustainable agriculture. Crop models are powerful tools to predict plant status when proper input information are provided. Remote sensing techniques are a unique way to acquire information on vegetation conditions over large areas to be used as forcing variables within simulation models. A field experiment was carried out in Lombardia, Northern Italy, in order to evaluate the potential of radiometric measurements for the prediction of rice nitrogen concentration for crop models forcing. The results indicate that rice reflectance is significantly influenced by nitrogen supply at certain wavelengths. Regression analysis highlighted that the visible region of the spectrum is the most sensitive to plant nitrogen concentration when reflectance measures are combined into a spectral index. An automated procedure allowed the analysis of all the possible wavelength combinations to derive a Normalized Difference Index (NDI) correlated to Plant Nitrogen Concentration (PNC). The derived index, which appeared to be least influenced by plant biomass and Leaf Area Index (LAI), and the Simple Ratio (SR) index, widely used as an indicator of vegetation conditions, have been spatialized over the experimental field. The output maps have been discussed in terms of ability in describing the spatial variability of Aboveground Biomass (AGB) and PNC.

Keywords: *Oryza sativa* L., proximal sensing, Vegetation Index, regression analysis

Riassunto

Lo sviluppo e la valutazione dell'effetto di pratiche agricole sostenibili si basa anche sulla disponibilità di strumenti e metodi per il monitoraggio delle condizioni delle piante coltivate e del loro stato nutrizionale. In questo contesto, i modelli agronomici sono uno strumento fondamentale per valutare lo stato delle piante purchè i dati in ingresso agli stessi siano adeguati ed attendibili. Il telerilevamento rappresenta uno strumento fondamentale per ottenere dati sulla vegetazione a scala territoriale; a questa scala, infatti, i metodi di indagine tradizionali richiederebbero risorse, sia in termini di tempo che di denaro, tali da rendere qualsiasi applicazione inattuabile. Il telerilevamento permette di derivare alcuni parametri caratteristici della vegetazione (es. indice di area fogliare e concentrazione di azoto nella pianta) che possono essere utilizzati nel forcing di modelli agronomici. In questo lavoro è stato condotto un esperimento di campo in Lombardia finalizzato a valutare l'utilità delle misure radiometriche per la stima della concentrazione di azoto nella pianta di riso per il forcing di modelli agronomici. I risultati indicano, innanzitutto, che la riflettività delle piante di riso è influenzata dalla quantità di azoto fornita durante la crescita e che, in particolare, si possono evidenziare alcune lunghezze d'onda dello spettro elettromagnetico dove questo effetto è particolarmente evidente. In particolare, è stata analizzata la correlazione tra la concentrazione di azoto e un indice spettrale normalizzato (Normalized Difference Index, NDI) derivato combinando le misure di riflettività in due lunghezze d'onda dello spettro; una procedura automatica ha permesso di correlare l'indice derivato con tutte le possibili combinazioni di lunghezze d'onda per individuare la combinazione che restituisse la massima correlazione. L'indice NDI così ottenuto ha dimostrato di essere poco influenzato sia da variazioni di biomassa sia di area fogliare; questo indice e il Simple Ratio (SR) sono stati spazializzati tramite tecniche di kriging sull'estensione totale del campo sperimentale. Le mappe così ottenute vengono discusse in questo articolo soprattutto in termini di abilità nella descrizione della variabilità in campo della biomassa e della concentrazione di azoto.

Parole chiave: *Oryza sativa* L., proximal sensing, indice di vegetazione, analisi di regressione

Introduction

Crop growth models simulate the time course of the main crop state variables (e.g. biomass, leaf area index, phenological stages) and of energy, carbon, water and nutrient fluxes at the crop/soil/atmosphere interfaces (Moulin *et al.*, 1998). Simulation models have been developed and applied mainly for crop yield forecasting

(food shortage early warning) (Supit *et al.* 1994; Bastiaansen and Ali, 2003; Yun, 2003; Doraiswamy *et al.*, 2005) and crop conditions assessment during the growing season (water and nitrogen deficit estimation). However, accurate and reliable model simulations depend on the availability of data on those environmental and man-

agement conditions that influence crop growth and development. These datasets, often available at field scale, are hardly available through expensive ground surveys at the regional or country levels with a satisfying temporal frequency and accuracy. At these scales of analysis, indeed, satellite and airborne imageries constitute a valuable source of spatially distributed information on the surface (soil and vegetation) conditions. Remotely Sensed (RS) data were first directly correlated to crop yield and they were exploited for crop production forecasting (Groten, 1993; Hayes and Decker, 1996); this approach was justified by the link observed between plant radiometric behaviour and its development and capability of absorbing radiation. However, more physically based approaches use radiometric data for the estimation of crop state variables such as Leaf Area Index (LAI [m^2m^{-2}]), the Fraction of Absorbed Photosynthetically Active Radiation (FAPAR) and canopy water content and structure (Moulin *et al.*, 1998; Doraiswamy *et al.*, 2005); these variables are directly responsible of the interaction between the vegetation and the radiation and therefore of the amount of energy measured by the sensor (Asrar *et al.*, 1989). Crop state variables can be derived from RS data by inverting radiative transfer models (e.g. Verhoef and Bach, 2003) or by formalising (semi-) empirical regressive relationships (e.g. Cohen *et al.*, 2003). Hence, quantitative variables derived from RS data can be integrated in crop growth models with the objective of strengthening their performance especially for regional monitoring.

The integration of RS data in crop growth models was first proposed by Wiegand *et al.* (1986) and several articles, published since then, describe the results of the integrated approach (Clevers *et al.*, 1994; Field *et al.*, 1995; Clevers and Leeuwen, 1996; Clevers *et al.*, 2002; Mo *et al.*, 2005). The integration can be performed in four different ways (Maas, 1988a, 1988b; Delécolle *et al.*, 1992; Moulin *et al.*, 1998):

1. Driving variables directly estimated from RS data;
2. State variables (e.g. LAI) updated with estimates derived from RS data;
3. Re-initialization of the model (i.e. adjustment of initial conditions to obtain simulations in agreement with RS-derived data);
4. Re-calibration (i.e. adjustment of the model's parameters to obtain simulations in agreement with RS-derived data).

The use of quantitative estimates from RS data to update state variables (II) is also called model *forcing*; that is, the model is forced to use the variable's value retrieved from the external source in order to provide the output simulation (Steven *et al.*, 1983; Leblon *et al.*, 1991; Clevers *et al.*, 2002). Literature review shows that the attention has been mainly focused on model forcing with RS-derived estimates of the key variables FAPAR (Leblon *et al.*, 1991; Clevers and van Leeuwen, 1996; Kiniry *et al.*, 2004) and LAI (Doraiswamy *et al.*, 2005). More recently, attention has been focused on Plant Nitrogen Concentration (PNC, hereafter always expressed as a percentage) assessment from RS data since Nitrogen (N) is a key factor in crop growth and often the major limiting nutrient in most agricultural soils. The direct

correlation between PNC and crop production is explained by the increased photosynthetic rate (Radiation Use Efficiency, RUE) as an effect of increased N availability (Sinclair and Horie, 1989; Hoesegawa and Horie, 1996); therefore, a crop growth model should take into account RUE variability as a function of PNC. The WARM development group (Confalonieri *et al.*, 2005) aims to integrate nitrogen dependent RUE for a better description of the processes governing rice plants growth. This article aims to describe a methodology for rice PNC estimation from RS data for a future integration in the WARM crop growth simulation model. In particular, the suitability of ground spectrometric data collected over an experimental field (proximal sensing technique) is evaluated as a basis for future applications at regional scale with airborne and satellite imageries.

The relationship between reflectance and plant nitrogen concentration

Remote sensing of agricultural resources is based on the measurement of the electromagnetic energy reflected or emitted from the Earth surface as a result of the energy-matter interaction. RS data interpretation and processing aim to derive vegetation biophysical properties (e.g. LAI, PNC, AGB) from its spectral properties (i.e. spectral signature).

Optical instruments, in particular, measure the amount of incoming solar radiation scattered back from the surface (i.e. reflectance factor) in the wavelength domain 350 nm to 2500 nm: Fig. 1 shows the reflectance factor as a function of the wavelength acquired over two vegetated surfaces (rice) with a field spectroradiometer (Field-Spec_FR PRO, ASD Inc., Boulder, Colorado, USA).

The canopy spectral signature, such as the one shown in Figure 1, is a function of the total leaf area, the geometry of the canopy (leaf angle distribution), the individual leaf optical properties (leaf spectral signature) and the back-

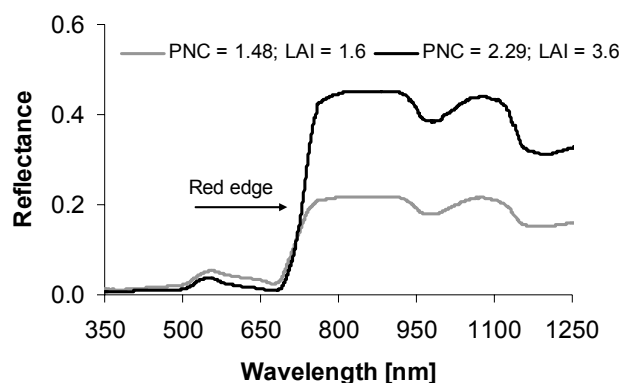


Fig. 1 - The canopy spectral signatures in the visible and near-infrared domains of the spectrum acquired over two experimental plots of rice (cv Gladio) grown under different fertilization treatments and characterised by different PNC and LAI.

Fig. 1 - Firme spettrali nelle lunghezze d'onda dello spettro visibile e vicino infrarosso acquisite per due parcelle del campo sperimentale (cv Gladio), dove il riso è cresciuto con diversi livelli di fertilizzazione e caratterizzate da diversi valori di LAI e concentrazione di azoto (PNC).

ground (either water or soil) reflectivity. Focusing on the visible (VIS, 350-700 nm) and near-infrared (NIR, 750-1250 nm) regions, the typical pattern of vegetation optical properties can be highlighted. The amount of radiation reflected from vegetation canopy in the VIS is quite low, due to the high absorption of radiation energy by the leaf pigments responsible of the photosynthetic process, primarily the chlorophylls, with a peak of reflectance in the green wavelengths (~550 nm) and a peak of absorption in the red wavelengths (~650 nm). In the NIR domain the reflectance factor is high due to both the high leaf reflectivity, caused by its internal cellular structure, and the enhancement of the reflectance caused by multiple radiation scattering between the canopy leaf layers. Finally, reflectance in the longer wavelengths of the NIR domain is mainly influenced by leaf water absorption thus reducing the reflectance factor. Between the red and NIR wavelengths (~715 nm), canopy reflectance is associated to the transition from chlorophyll absorption processes to leaf and within-leaf scattering; this position is identified by the wavelength of maximum slope of the reflectance spectrum between 650 nm and 800 nm (Munden *et al.*, 1994) often referred to as *red edge*. As chlorophyll concentration increases the absorption feature in the red region broadens, and the red edge position shifts towards longer wavelengths.

The potential of remotely sensed data relies on the above-described dependence of the vegetation spectral signature on biophysical properties. PNC can be estimated from remotely sensed data thanks to its correlation with chlorophyll pigments (Yoder and Pettigrew-Crosby, 1995), which are responsible of the interaction with radiation and, hence, of the vegetation optical properties. Changes in leaf chlorophyll concentration produce rather broad-band differences in leaf reflectance and transmittance spectra. However, the transition from leaf spectra to canopy reflectance is complicated (Daughtry *et al.* 2000).

The reflectance measured in correspondence of two or more wavelengths can be combined in a spectral Vegetation Index (VI) that can synthesize multi-spectral information and can be correlated to vegetation biophysical variables. Moreover, VIs can be specifically developed to enhance the sensitivity to the variable of interest (e.g. chlorophyll concentration) and to reduce undesired effects such as the influence of the background reflectance. The correlation between VIs and PNC can be exploited to derive a regressive model that allows the estimation of PNC from measured VIs (Stroppiana *et al.*, 2005). The Normalized Difference Vegetation Index (NDVI) has been widely used for vegetation monitoring primarily for its simplicity. It is conceived as the normalized difference between the minimum peak of reflectance in the red wavelengths and the maximum reflectance in the NIR domain ($NDVI = (\rho_{NIR} - \rho_{RED}) / (\rho_{NIR} + \rho_{RED})$): the higher the index value the better the vegetation conditions in terms of both biomass amount and vegetation health. A wide range of vegetation/spectral indices have been developed and applied for chlorophyll and nitrogen content estimation (e.g. Daughtry *et al.*, 2000; Haboudane *et al.*, 2002), although the improvements brought by the increased complexity of the indices appear dependent on the condi-

tions of application. For instance, Daughtry *et al.* (2000) showed that the Modified Chlorophyll Absorption Reflectance Index (MCARI), specifically developed for chlorophyll estimation, is more influenced by canopy structure (i.e. LAI) than pigment concentration.

Agronomic and spectrometric field data

Ground data were collected in the framework of a field experiment carried out in 2004 in Opera, south of Milano, Italy. The experimental site was composed of 40 7x5 m² plots where Gladio (Indica type) and Volano (Japonica type) rice cultivars were sown on May 24 in a completely randomized block design with four replicates. Rice was grown under flooded conditions. Five different fertilization levels were applied for each cultivar by top-dressing nitrogen fertilization (urea): a reference condition in which rice was let grow with no additional fertilizer (N0) and four additional levels, where N was applied differently at two times during the crop cycle (beginning of tillering, June 22, and panicle initiation, July 20) (N1: 40+40 kg ha⁻¹; N2: 80+80 kg ha⁻¹; N3: 40+0 kg ha⁻¹; N4: 0+80 kg ha⁻¹). Ground canopy reflectance data were acquired with a FieldSpec_FR PRO (FS) spectroradiometer with a quasi-weekly time step (number of sampling dates, n=8) from beginning of tillering to the end of stem elongation phase corresponding to codes 25 and 34 of the BBCH scale of rice (Lancashire *et al.*, 1991), respectively. The FS instrument provides reflectance measurements in the 350 to 2500 nm spectral range with a 4 nm spectral resolution and a 1 nm sampling step (hyperspectral radiometer). Spectral measurements were collected above the canopy in correspondence of five positions within each plot (four at the corners and one at the centre) in order to cover the entire plot's area. LAI was measured with both destructive and indirect methods (Jonckheere *et al.*, 2004; Weiss *et al.*, 2004). The direct destructive measurements were performed by sampling rice plants in the field and by measuring the leaf area in laboratory through digital photography. The indirect non destructive measurements were performed with a LAI2000 instrument (LI-COR, Inc., Nebraska, USA) along a transect composed of two above and four below canopy readings within each plot. LAI values were derived by post processing the instrument output discarding the last ring readings (Stroppiana *et al.*, 2006). Measurements were extended until maximum LAI was reached (n=11).

Eight sample plots (four replicates for fertilization levels N0 and N2 for the Gladio cv.) were monitored by measuring AGB, PNC, and LAI (direct method) at the same time, when feasible, of the spectroradiometric measurements (n=6). Optimal sample size was determined for each plot using the visual jackknife method (Confalonieri, 2004; Confalonieri *et al.*, 2006). AGB was determined by storing the samples in oven at 105 °C until constant weight and PNC by using an elementary analyzer (CE 1500 NA, Carlo Erba, Milano, Italy). In this study we present results from the analyses of the nitrogen concentration and spectroradiometric ground measurements in the eight sample plots. Hence, results are limited to the Gladio cv. and the two fertilization levels N0 and N2.

Methodology

In order to investigate the relationship between PNC and canopy reflectance, the mean spectral signature derived from the five measurements acquired over each plot has been correlated to the average PNC measured for the sampled plants for the eight plots monitored. A total of 48 couples of values (8 plots x 6 dates) were available for the regression analysis. Univariate ordinary least square regression analysis was first applied to investigate the correlation between the canopy reflectance (ρ_{λ_i}) measured at each wavelength (λ_i) of the FS instrument and PNC; the objective is to highlight those spectral regions sensitive to PNC by exploiting the hyperspectral property of the field sensor.

Since vegetation/spectral indices are commonly used for vegetation monitoring, we also quantified the correlation between a Normalized Difference Index (NDI) (Equation 1) and PNC.

$$NDI = \left(\frac{\rho_i - \rho_j}{\rho_i + \rho_j} \right) \quad (1)$$

Rather than selecting an *a-priori* couple of wavelengths (λ_i , λ_j) to be combined in the spectral index, by exploiting again the hyperspectral characteristics of the radiometric dataset, all the possible combinations of spectral bands (λ_i , λ_j) were analysed to identify the combination that provides the highest correlation with PNC. The relationship between vegetation/spectral indices and biophysical variables is generally of a logarithmic type describing a typical VI saturation effect in the presence of dense canopy or high pigment concentration (Carlson and Ripley, 1997; Hanna *et al.*, 1999; Boschetti *et al.*, 2006); all the results presented in the following sections refer to a logarithmic relationship. The index derived with the selected spectral bands is the optimal index for PNC estimation (NDI_{opt}) among those computable with any other combination of bands. The index of the form shown in Equation 1 coincides with the NDVI when the ρ_{λ_j} , ρ_{λ_i} are selected in the red and near infrared domains of the spectrum, respectively.

The correlation between spectrometric data and biophysical variables were similarly performed for the LAI and AGB datasets. These analyses aimed to verify whether the regions of the spectrum and the indices suitable for LAI and AGB estimation are significantly different with respect to those selected for PNC assessment. Indeed, an index optimal for PNC estimation should be least influenced by the variability of factors other than the PNC.

Finally, NDI_{opt} and the Simple Ratio ($SR = \rho_{\lambda_j} / \rho_{\lambda_i}$; where $\lambda_j = 800$ nm and $\lambda_i = 670$ nm) indices were mapped over the experimental site using spatialisation algorithms (kriging) implemented in the Surfer Version 8.0 (Golden Software, Inc.) software. The SR index has been widely used as an indicator of vegetation vigour (i.e. biomass) (Jordan, 1969) and it has been preferred to the NDVI, which showed significant saturation behaviour (Carlson and Ripley, 1997). In fact, the NDVI values measured at the experimental site reached the top of the index range

(NDVI > 0.9) even at the beginning of the experimental measurements.

Results and discussion

Figure 2 shows the results of the regression analysis: the Pearson coefficient of linear correlation (r) is plotted as a function of the wavelength to quantify the relationship between reflectance and PNC, LAI and AGB and to highlight the direction of this relationship. The graph was limited to the 350-950 nm spectral range due to the low S/N ratio that characterises longer wavelengths in the short-wave infrared domain.

The reflectance measured by the instrument is greatly influenced by the canopy structural parameters (LAI and AGB) in both the visible (VIS) and near-infrared (NIR) spectral domains ($r^2_{PNC} < 0.30$; $r^2_{LAI} < 0.74$; $r^2_{AGB} < 0.84$). Nevertheless, the correlation with PNC in the VIS is higher compared to values estimated in the NIR, according to previous findings which showed that light absorption by chlorophyll dominates the leaf spectral properties in the blue (~450 nm) and red (~670 nm) wavelength regions (Chappelle *et al.*, 1992; Daughtry *et al.*, 2000). This effect is significantly reduced at the canopy level where, besides leaf properties, structural parameters play a key role in the interaction with incoming solar radiation especially in the NIR (>750 nm) region where leaf reflectance is not related to leaf chlorophyll but to leaf structure (Knipling, 1970). For example, Daughtry *et al.* (2000) quantified that as much as 87.7% of the variation in canopy reflectance at 801 nm is due to variations in LAI.

Moreover, the two regions of the spectrum show opposite behaviours (Figure 2): the NIR wavelengths are inversely related to PNC and positively related to LAI and AGB, the opposite occurs in the VIS.

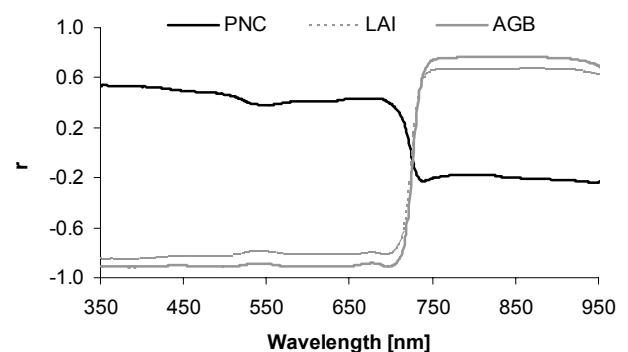


Fig. 2 - The Pearson coefficient of linear correlation (r) as a function of the wavelength for rice PNC, LAI and AGB ($n=48$). The biophysical variable were transformed in logarithmic scale for the regression analysis.

Fig. 2 - Andamento del coefficiente di correlazione lineare di Pearson (r) in funzione della lunghezza d'onda per i parametri concentrazione di azoto, indice di area fogliare e biomassa ($n=48$). Le variabili biofisiche sono state trasformate secondo la funzione logaritmica.

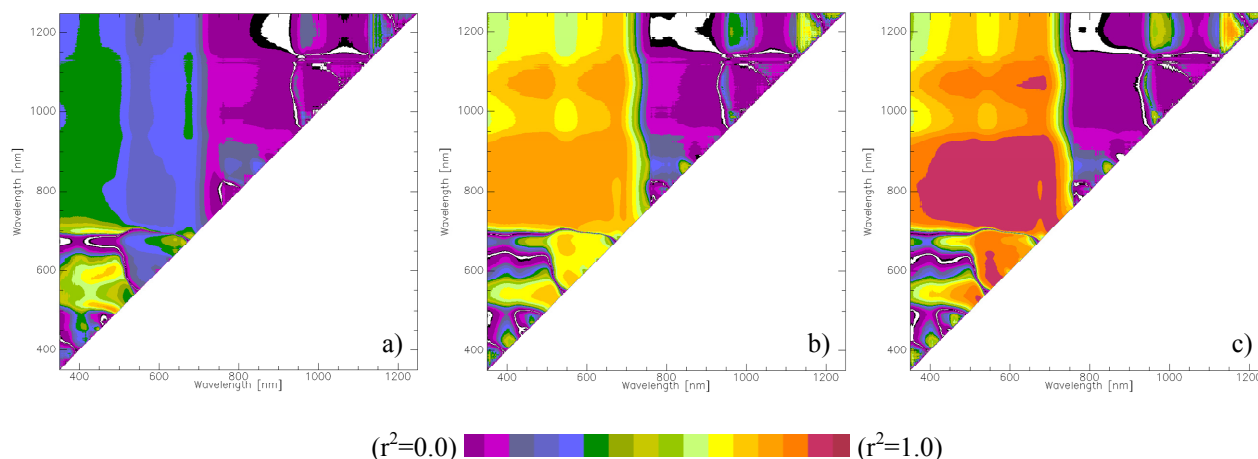


Fig. 3 - The coefficient of determination (r^2) computed between PNC (panel a), LAI (panel b) and AGB (panel c) measurements and the NDI ($n=48$) obtained with all the possible combination of bands in the range of acquisition of the FS instrument. The figure shows only the 350-1250 nm VIS-NIR range.

Fig. 3 - Valori del coefficiente di determinazione (r^2) calcolato per regressione tra l'indice NDI, ottenuto con tutte le possibili combinazioni di lunghezze d'onda nel range dello strumento FS, e la concentrazione di azoto (PNC) (a), il LAI (b) e la biomassa (AGB)(c) ($n=48$). La figura presenta solo i risultati nel range del visibile e dell'infrarosso vicino (350-1250 nm).

Figure 2 also highlights the position of the Red Edge wavelength (~725 nm) where r^2 is equal to 0 for all variables. No spectral region can be identified where reflectance is correlated to N concentration better than to LAI or AGB. The results presented here show that it is clearly necessary to reduce the influence of these parameters before attempting to estimate rice PNC at canopy level. Daughtry *et al.* (2000) found that attempts to assess plant N status based on canopy reflectance in a single band often will be confounded by the variability in background reflectance and/or LAI. On the contrary, ratios or more complex wavebands combinations (vegetation/spectral indices) greatly improve the low performance of a single wavelength approach, shown by Figure 2, by minimizing the influence of extraneous factors and maximizing the sensitivity to the variable of interest. Figure 3.a shows the correlation between rice PNC and the NDI index for each couple of wavelengths of the VIS-NIR domain.

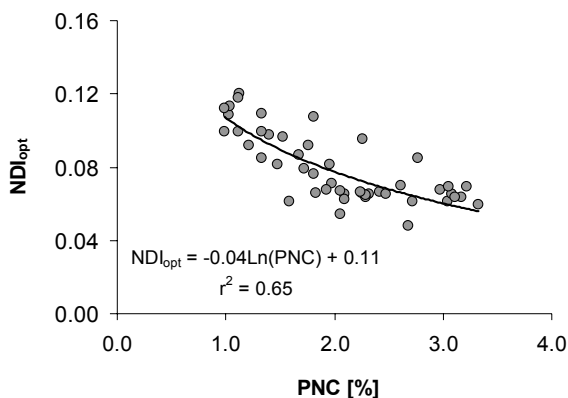


Fig. 4 - The correlation between NDI_{opt} and PNC.
Fig. 4 - La correlazione tra NDI_{opt} e la concentrazione di azoto (PNC).

As already pointed out above, the VIS is the most suited region of the spectrum for PNC estimation and the use of a combination of bands improved the correlation with measured PNC. The highest correlation ($r^2=0.65$) is obtained from the combination of the reflectance factors in two bands in the visible region: $\lambda_i=503$ nm and $\lambda_j=483$ nm. The correlation between the index obtained with these two wavelengths (NDI_{opt}) and PNC is shown in Figure 4: an inverse logarithmic relationship exists between the two variables.

The results of the same type of regression analysis performed with the LAI and AGB datasets are shown in Figures 3.b and 3.c, respectively. The highest r^2 values for these two variables are obtained when the bands combined into the NDI are chosen in the NIR region of the spectrum ($\lambda > 700$ nm). In particular, in the case of AGB the coefficient of determination reaches the highest values ($r^2 > 0.9$) thus confirming that the NDVI-type indices are highly correlated to the amount of biomass. On the contrary, the lowest correlation is achieved when reflectance measured in the VIS is exploited to derive the index. If the same wavelength combination ($\lambda_i=503$ nm, $\lambda_j=483$ nm) found to be the most suited for PNC estimation is used in the NDI, the r^2 computed for LAI and AGB is 0.31 and 0.27, respectively. In a multivariate regression analysis with NDI_{opt} as dependent variable and logarithmic transformed PNC, LAI and AGB as independent variables, only the regression coefficient relative to PNC is statistically significant ($***P < 0.001$). This result further confirms that the index is least influenced by LAI and AGB.

Since the major advantage of remotely sensed data is the ability in providing spatially distributed information, we spatialized the NDI_{opt} and the SR indices. We pointed out that different indices can highlight different properties of the vegetated surfaces hence the maps, derived from the spatialization over the experimental field, are expected to highlight independent patterns related to either LAI/AGB

or PNC. Figure 5 shows the SR and NDI_{opt} maps derived over the field for four dates during the crop cycle.

Note that, besides the two fertilization levels monitored (N0 and N2), there are three more levels within the experimental field that contribute to the spatial pattern highlighted in the figure. Both the VIs in the figure show an increasing level of spatial variability due to different growing conditions of the rice plants. The lowest variability in the SR values in the field is on June 25, a month after sowing and 5 days after the first fertilization, which occurred on June 22. On the same date, the NDI_{opt} values show a higher rate of variability compared to SR probably due to more variable nitrogen concentration as a consequence of the first fertilization and of different initial soil conditions. The homogeneity shown at the beginning of the crop cycle is progressively lost and it drastically decreases after the second fertilization supplied on July 20. The figure clearly shows the effect of the second fertilization on both the indices. The highest values of biomass (high SR, orange to red colours) and nitrogen concentration (low NDI_{opt}, orange and red colours) in most cases occur in the most fertilized plots of the second treatment (dark grey filled cells). In the case of SR, this correspondence is already evident in the results derived for July 28 (8 days after the second fertilization) but it becomes clearer for August 16 when almost all the plots show an increase of the SR values; this increase is likely due to the increased AGB. On the contrary, the NDI_{opt} map on July 28 shows a good correspondence between the highest levels of fertilization and the highest levels of nitrogen (lowest NDI_{opt}) but on August 16 the N levels are generally decreased probably due to the N dilution by the rice plants. Indeed AGB is characterised by a monotonic increase with time and PNC by a curve with maximum peaks after the fertilization treatments.

Figure 6 shows the mean NDI_{opt} (panel a) and SR (panel b) for the four fertilization treatments of the experimental field. Note that NDI_{opt} and PNC are inversely related, as shown by Figure 4, and therefore the lowest index values identify the highest N concentration in rice plants. Before the second fertilization, the values of both the indices do not differentiate significantly among treatments. No significant statistical differences have been found among treatments for the field AGB and PNC measurements. However, the greater proximity of the mean NDI_{opt} curves suggests that, in terms of PNC, plots' conditions might be more homogeneous. Apparently, the first fertilization treatment had a greater effect on plants AGB, rather than PNC, especially in the case of the highest fertilized plots (triangular markers in Figure 6.b). After the second fertilization (highlighted in the figure by a black arrow), NDI_{opt} decreases and SR increases significantly according to measurements acquired on July, 28; it is probable that the field campaign carried out on July 22 was too close to the treatment to highlight an effect on plants' conditions. The last campaign (August 16) clearly shows how the plots cluster in two groups based on whether or not they were fertilized a second time.

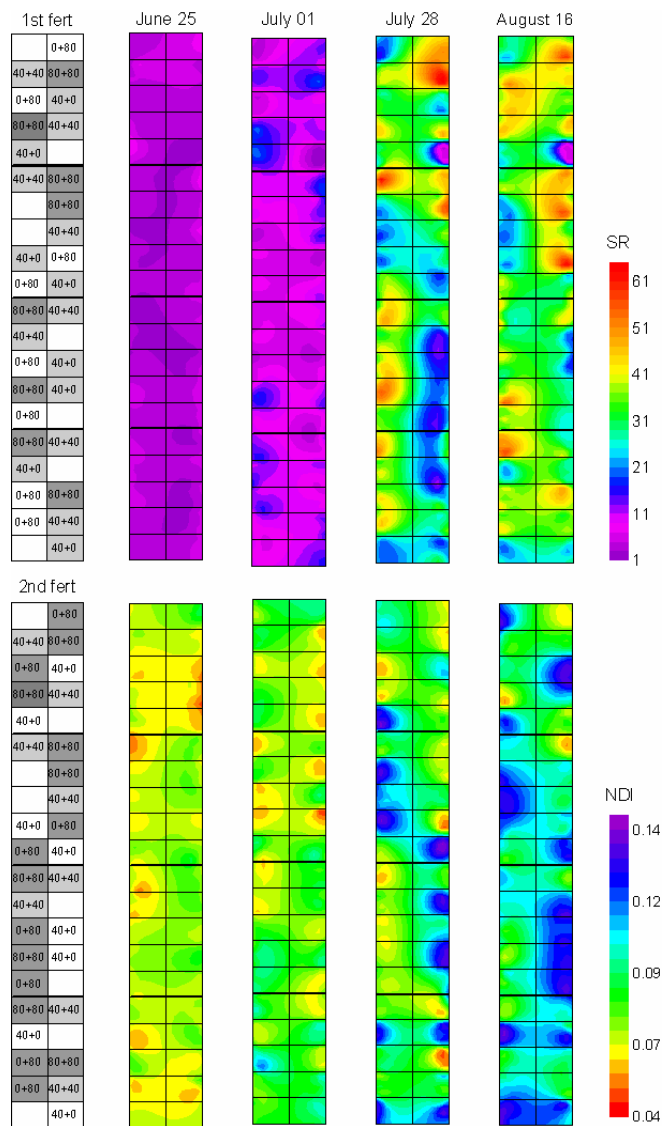


Fig. 5 - SR and NDI_{opt} maps over the experimental field. The colour scale of the NDI_{opt} index has been inverted to better represent its inverse proportionality with PNC (see Fig. 4). The first column shows the amount of fertilizer supplied at the first (top) and second (bottom) fertilization treatments as filled grey levels (white, light grey and dark grey indicate 0 kg ha⁻¹, 40 kg ha⁻¹ and 80 kg ha⁻¹, respectively); the total amount supplied to each plot is also shown by the text label within each cell ([kg ha⁻¹]).

Fig. 5 - Mappe degli indici SR e NDI_{opt} per il campo sperimentale. La scala di colori dell'indice NDI_{opt} è stata invertita per meglio rappresentare la sua relazione di inversa proporzionalità rispetto a PNC (vedi Figura 4). La prima colonna mostra la quantità di azoto fornita nella prima (in alto) e nella seconda (in basso) fertilizzazione. I diversi livelli di fertilizzazione sono rappresentati da diversi toni di grigio (bianco, grigio chiaro e grigio scuro indicano, rispettivamente, 0 kg ha⁻¹, 40 kg ha⁻¹ and 80 kg ha⁻¹). La quantità totale di azoto fornita ad ogni parcella è invece indicata dall'etichetta all'interno di ogni cella.

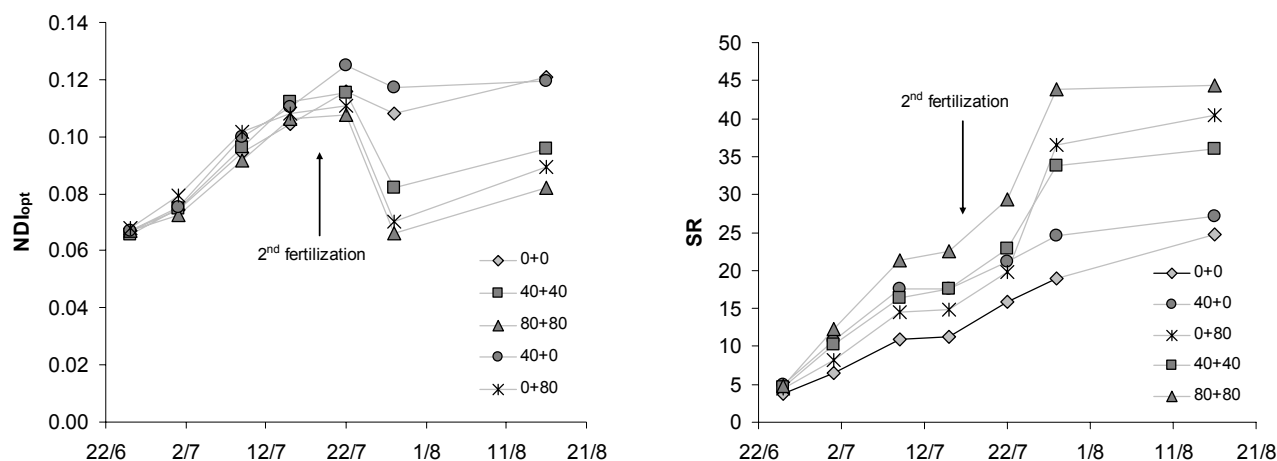


Fig. 6 - The mean NDI_{opt} (panel a) and SR (panel b) for the four fertilization treatments of the experimental field.

Fig. 6 - Andamento temporale degli indici NDI_{opt} (a) e SR (b) medi per i quattro livelli di fertilizzazione del campo sperimentale.

Conclusions

Remote sensing techniques are a unique tool for frequent and non destructive vegetation conditions assessment over large areas, as required by agriculture monitoring. The radiometric properties of the vegetated surfaces are correlated to biophysical variables among which Plant Nitrogen Concentration (PNC), Leaf Area Index (LAI) and Aboveground Biomass (AGB), that constitute key input data for crop growth models. This study investigates the ability of a single band and of band combinations (Normalized Difference Index, NDI) to PNC assessment by univariate regression analysis of field measurements (laboratory plant nitrogen estimates and spectrometric data acquired with proximal sensing techniques). The analysis of the correlation between single band reflectance and N concentration confirms previous findings and showed a weak prediction ability over the visible and near-infrared spectrum range. Besides the low coefficient of determination, the reflectance is also highly affected by canopy biomass and leaf area.

In the case of an NDI index, all the possible band combinations have been screened with the objective of seeking the couple of bands that combined into the index provide the highest correlation with PNC measurements. This approach exploited the hyperspectral property of the spectroradiometer used for field data acquisition. The two wavelengths found to provide the highest correlation ($r^2=0.65$) between the index and PNC belong to the visible blue/green region of the electromagnetic spectrum: $\lambda_i=503$ nm and $\lambda_j=483$ nm. The relationship between the index and PNC can be inverted to derive an estimate of PNC from data acquired with proximal and remote sensing techniques thus providing input data for a regional application of crop growth models such as WARM.

The same procedure has been applied to the LAI and AGB field datasets; the results showed that the reflectance measured in the NIR rather than VIS region of the electromagnetic spectrum can be correlated to these two variables. These results suggest that the index derived for PNC assessment (NDI_{opt}) is least influenced by LAI and AGB.

The NDI_{opt} and a Simple Ratio (SR) index have been spatialized over the experimental field to picture the variability of N concentration and biomass to which the indices are, respectively, correlated. The output maps confirm previous results: indeed, they show different patterns due to a different spatial variability of the biophysical variables. These maps, obtained with proximal sensing techniques, highlight the potential of radiometric (remotely and proximal sensed) data for regional vegetation monitoring. Based on these results derived with a hyperspectral dataset, satellite data (either simulated or acquired) will be used to further investigate the relationship with PNC for future applications that exploit the commercial available datasets.

Moreover, the relationship between nitrogen and chlorophyll concentration will be further analysed. Chlorophyll is the actual responsible of the interaction between canopy and solar radiation. Although it is well known that a nitrogen deficiency determines a reduction of chlorophyll pigments, a more detailed investigation of the relationship between these two variables and the possibility of using this kind of information to force models would greatly improve models performance, especially for large scale simulations.

Acknowledgements

The authors would like to thank all those people who contributed with their work during the field campaigns. This publication has been partially funded under the TOPFERT exploratory research project funded by the Institute for the Protection and Security of the Citizen, Joint research Centre of the European Commission

References

- Asrar, G., Myneni, R.B., Kanemasu, E.T., 1989. Estimation of plant canopy attributes from spectral reflectance measurements. In: Asrar, G. (Ed.), *Theory and Applications of Optical Remote Sensing*. Wiley Interscience, 252-292.
- Bastiaanssen, W.G.M., Ali, S., 2003. A new crop yield forecasting model based on satellite measurements applied across the Indus basin, Pakistan. *Agriculture, Ecosystems & Environment*, 94, 321-340.
- Boschetti, M., Bocchi, S., Brivio, P.A., 2007. Assessment of pasture production in the Italian Alps using spectrometric and remote sens-

- ing information. *Agriculture, Ecosystems and Environment*, 118, 267-272.
- Carlson, T.N., Ripley, D.A., 1997. On the relation between NDVI, fractional and vegetation cover, and the leaf area index. *Remote Sensing of Environment*, 62, 241-252.
- Chappelle, E.W., Kim, M.S., McMurtrey, J.E., 1992. Ratio analysis of reflectance spectra (RARS): an algorithm for remote estimation of the concentrations of chlorophyll a, chlorophyll b, and carotenoids. *Remote Sensing of Environment*, 39, 239-247.
- Clevers, J.G.P.W., Vonder, O.W., Jongschaap, R.E.E., Desprats, J-F., King, C., Prévot, L., Bruguier, N., 2002. Using SPOT data for calibrating a wheat growth model under Mediterranean conditions. *Agronomie*, 22, 687-694.
- Clevers, J.G.P.W., Van Leeuwen, H.J.C., 1996. Combined use of optical and microwave remote sensing data for crop growth monitoring. *Remote Sensing of Environment*, 56, 42-51.
- Clevers, J.G.P.W., Bùker, C., Van Leeuwen, H.J.C., Bouman, B.A.M., 1994. A framework for monitoring crop growth by combining directional and spectral remote sensing information. *Remote Sensing of Environment*, 50, 161-170.
- Cohen, W.B., Maieresperger, T.K., Gower, S.T., Turner, D.P., 2003. An improved strategy for regression of biophysical variables and Landsat ETM+ data. *Remote Sensing of Environment*, 84, 561-571.
- Confalonieri, R., 2004. A jackknife-derived visual approach for sample size determination. *Rivista Italiana di Agrometeorologia*, 1, 9-13.
- Confalonieri, R., Acutis, M., Donatelli, M., Bellocchi, G., Mariani, L., Boschetti, M., Stroppiana, D., Bocchi, S., Vidotto, F., Sacco, D., Grigani, C., Ferrero, A., Genovese, G., 2005. WARM: a scientific group on rice modelling. *Rivista Italiana di Agrometeorologia*, 2, 54-60.
- Confalonieri, R., Stroppiana, D., Boschetti, M., Gusberty, D., Bocchi, S., Acutis, M., 2006. Analysis of rice sample size variability due to development stage, nitrogen fertilization, sowing technique and variety using the visual jackknife. *Field Crops Research*, 97, 135-141.
- Daughtry, C.S.T., Waithall, C.L., Kim, M.S., de Colstoun, E.B., McMurtrey III, J.E., 2000. Estimating corn leaf chlorophyll concentration from leaf and canopy reflectance. *Remote Sensing of Environment*, 74, 229-239.
- Delécolle, R., Maas, S. J., Guérif, M., Baret, F., 1992. Remote sensing and crop production models: present trends. *ISPRS Journal of Photogrammetry and Remote Sensing*, 47, 145-161.
- Doraiswamy, P.C., Sinclair, T.R., Hollinger, S., Akhmedov, B., Stern, A., Prueger, J., 2005. Application of MODIS derived parameters for regional crop yield assessment. *Remote Sensing of Environment*, 97, 192-202.
- Field, C.B., Randerson, J.T., Malmström, C.M., 1995. Global Net Primary Production: combining ecology and remote sensing. *Remote Sensing of Environment*, 51, 74-88.
- Groten, S.M.E., 1993. NDVI-crop monitoring and early yield assessment of Burkina Faso. *International Journal of Remote Sensing*, 14, 1495-1515.
- Haboudane, D., Miller, J.R., Tremblay, N., Zarco-Tejada, P.J., Dextraze, L., 2002. Integrated narrow-band vegetation indices for prediction of crop chlorophyll content for application to precision agriculture. *Remote Sensing of Environment*, 81, 416-426.
- Hanna, M.M., Steyn-Ross, D.A., Steyn-Ross, M., 1999. Estimating biomass for New Zealand pasture using optical remote sensing techniques. *Geocarto International*, 14(3), 89-94.
- Hayes, M.J., Decker, W.L., 1996. Using NOAA-AVHRR data to estimate maize production in the United States corn belt. *International Journal of Remote Sensing*, 17, 3189-3200.
- Hosegawa, T., Horie, T., 1996. Leaf nitrogen, plant age and crop dry matter production in rice. *Field Crops Research*, 47, 107-116.
- Jonckheere, I., Fleck, S., Nackaerts, K., Muys, B., Coppin, P., Weiss, M., Baret, F., 2004. Review of methods for in-situ leaf area index determination. Part I. Theories, sensors and hemispherical photography. *Agric. For. Meteorol.* 121, 19-35.
- Jordan, C.F., 1969. Derivation of leaf-area index from quality of light on the forest floor. *Ecology*, 50, 663-666.
- Kiniry, J.R., Bean, B., Xie, Y., Chen, P., 2004. Maize yield potential: critical processes and simulation modeling in a high-yielding environment. *Agricultural Ecosystems*, 82, 45-56.
- Knipling, E.B., 1970. Physical and physiological basis for the reflectance of visible and near-infrared radiation from vegetation. *Remote Sensing of Environment*, 1, 155-159.
- Lancashire, P.D., Bleiholder, H., Langelüddecke, P., Stauss, R., Van de Boom, T., Weber, E., Witzemberger, A., 1991. A uniform decimal code for growth stages of crops and weeds. *Annals of Applied Biology*, 119, 561-601.
- Leblon, B., Guérif, M., Baret, F., 1991. The use of remotely sensed data in estimation of PAR use efficiency and biomass production of flooded rice. *Remote Sensing of Environment*, 38, 147-158.
- LI-COR, 1991. LAI-2000 Plant Canopy Analyser Operating Manual. LI-COR, Inc. Lincoln, Nebraska, USA.
- Maas, S. J., 1988a. Use of remotely-sensed information in agricultural crop growth models. *Ecological Modelling*, 41, 247-268.
- Maas, S. J., 1988b. Using satellite data to improve model estimates of crop yield. *Agronomy Journal*, 80, 655-662.
- Mo, X., Liu, S., Lin, Z., Xu, Y., Xiang, Y., McVicar, T.R., 2005. Prediction of crop yield, water consumption and water use efficiency with SVAT-crop growth model using remotely sensed data on the North China Plain. *Ecological Modelling*, 183, 301-322.
- Moulin, S., Bondeau, A., Delécolle, R., 1998. Combining agricultural crop models and satellite observations: from field to regional scales. *International Journal of Remote Sensing*, 19, 1021-1036.
- Munden, R., Curran, P.J., Catt, J.A., 1994. The relationship between red edge and chlorophyll concentration in the Broad-balk winter wheat experiment at Rothamsted. *International Journal of Remote Sensing*, 15, 705-709.
- Sinclair, T.R., Horie, T., 1989. Leaf nitrogen, photosynthesis, and crop radiation use efficiency: A review. *Crop Science*, 29, 90-98.
- Steven, M.D., Biscoe, P.V., Jaggard, K.W., 1983. Estimation of sugarbeet productivity from reflection in the red and infrared spectral bands. *International Journal of Remote Sensing*, 4, 325-334.
- Stroppiana D., Boschetti, M., Confalonieri, R., Bocchi, S., Brivio, P.A., 2005. Analysis of hyperspectral field radiometric data for monitoring nitrogen concentration in rice crops. *Proceedings of SPIE, Remote Sensing for Agriculture, Ecosystems and Hydrology*, 20-22 September 2005, Bruges, Belgium, Owe, M., D'Urso, G. (Eds), SPIE Vol. 5976, 59760R-1-9.
- Stroppiana D., Boschetti, M., Confalonieri, R., Bocchi, S., Brivio, P.A., 2006. Evaluation of LAI-2000 for leaf area index monitoring in paddy rice. *Field Crops Research*, 99, 167-170.
- Supit, I., Hooijer, A.A., Van Diepen, C.A., 1994. System description of the WOFOST 6.0 crop simulation model implemented in CGMS, Theory and algorithms. *An Agricultural Information System for the European Community*, Vol. 1, EUR 15956 EN, 144 pp.
- Verhoef, W., Bach, H., 2003. Remote sensing data assimilation using coupled radiative transfer models. *Physics and chemistry of the Earth, Parts A/B/C*, 28, 3-13.
- Weiss, M., Baret, F., Smith, G.J., Jonckheere, I., Coppin, P., 2004. Review of methods for in-situ leaf area index (LAI) determination: Part II. Estimation of LAI, errors and sampling. *Agriculture and Forestry Meteorology* 121, 37-53.
- Wiegand, C. L., Richardson, A. J., Jackson, R. D., Pinter, P. J. Jr, Aase, J. K., Smika, D. E., Lautenschlager, L. F., McMurtrey III, J. E., 1986. Development of agrometeorological crop model inputs from remotely sensed information. *IEEE Transactions on Geoscience and Remote Sensing*, 24, 90-97.
- Yoder, B.J., Pettigrew-Crosby, R.E., 1995. Predicting nitrogen and chlorophyll content and concentrations from reflectance spectra (400-2500 nm) at leaf and canopy scales. *Remote Sensing of Environment*, 53, 199-211.
- Yun, J.I., 2003. Predicting regional rice production in South Korea using data and crop-growth modelling. *Agricultural Systems*, 77, 23-38.